12th International Conference on Fracture Mechanics of Concrete and Concrete Structures
FraMCoS-12
B.L.A. Pichler, Ch. Hellmich, P. Preinstorfer (Eds)

https://doi.org/10.21012/FC12.1235
MS07-3:1

COMPARISON OF BOND STRENGTH TO AGGREGATE BETWEEN REACTIVE MAGNESIA CEMENT (RMC) AND PORTLAND CEMENT (PC)

Wu Bo*, Wang Tianyu* and Qiu Jishen*

* Department of Civil and Environmental Engineering, Hong Kong University of Science and Technology, 1 University Road, Clear Water Bay, Hong Kong, China
e-mail:wubo@ust.hk, cejqiu@ust.hk

Key words: Reactive magnesia cement, cement-aggregate bond strength, carbonation, microstructure.

Abstract: The aggregate-cement paste bond strength is one of crucial factors influencing the durability, overall mechanical performance and lifespan of concrete. This study for the first time compared the bond strength to aggregate between reactive magnesium cement (RMC) and traditional Portland cement (PC). The mechanical properties, including compression strength and bond strength, of RMC highly rely on the carbonation curing while carbonation curing slightly reduces the mechanical properties of PC. Even though under carbonation curing, the bond strength of RMC is still inferior to the PC, which is due to limited carbonation depth, as evidenced by XRD and TGA characterizations. The contribution of carbonation to the bond strength was calculated, showing that the RMC holds great potential to achieve greater bond strength compared with PC if the carbonation degree can be further increased.

1 INTRODUCTION

Reactive magnesium cement (RMC) shows great promise as an eco-friendly substitute for the Portland cement (PC) because of its excellent potential to sequester CO_2 through mineralization and its full recyclability at the end of life [1, 2]. The carbonation of brucite, originates from the MgO hydration, enables the permanent storage of CO_2 via the formation of a variety of hydrated magnesium carbonates (HMCs). The conversion of brucite into HMCs is a process of solid volume expansion by a factor of 1.8-3.1, which leads to a significant densification of microstructure and strength development [3]. By introducing the hydration agent (e.g., magnesium acetate [4]) and nucleation seeds (e.g., hydromagnesites [5]), the hydration of MgO and carbonation process could be expedited, leading to an improved compression strength of up to around 70 MPa. In addition, the incorporation of minor natural fibers prominently boosted the CO_2 diffusion and carbonation of RMC, elevating the compression strength up to 92 MPa [6].

The interface transition zone (ITZ) between aggregate and cement paste is one of critical factors determining the mechanical performance, resistance, and durability of concrete. The bond strength between aggregate and cement paste is highly associated with the mechanical interlocking derived from the epitaxic growth of cement hydration products on aggregated surface and chemical reactions between aggregate and cement paste [7, 8]. In PC-based concrete, the bond strength between aggregate and cement paste was extensively investigated, including the aggregate type [9], aggregate surface roughness [10], recycled aggregate [11], mix proportions of cement paste [12], and effects of nanofillers [13]. By

comparison, the performances of RMC-based concrete were rarely reported. Pan et al. [2] and Pu et al. [14] investigated the mechanical performance and carbonation products of RMC with recycled aggregate, revealing that the porous ITZ between recycled aggregate and RMC could facilitate the CO_2 diffusion and strength gain. However, the bond strength between aggregate and RMC is still out of existing studies.

This work for the first time compared the bond strength to aggregate between RMC and PC under carbonation curing and sealed curing. The carbonation profile of cement paste was detected by XRD and TGA analysis. Finally, the relationship between carbonation degree of cement paste and bond strength was discussed.

2 EXPERIMENTAL PROGRAMS

The mix proportions of RMC and PC-based cement paste are listed in **Table 1**. To achieve the comparable flowability, the water-binder ratio is 0.76 for RMC, while that of PC is 0.32. PVA fibers were added to cement paste to improve volume stability and avoid rupture of cement paste under tensile loading.

To determine the aggregate-cement paste bond strength, the polished basalt rock with the dimension of ϕ 50×50 mm^3 was fixed in the bottom of mold with the dimension of ϕ 50×100 mm^3. Then the fresh composites were cast on the top of basalt rock and covered with plastic membrane. In addition, the 40 mm^3 cubes were used to test the compression strength of cement matrix. After 24 hours curing under ambient environment, the hardened specimens were demoulded and divided into two groups: one group was cured in a sealed plastic bag; other group was moved to carbonation chamber (30±2 °C, R.H. of 85±5%, CO_2 concentration of 10%).

Unconfined uniaxial compression tests were conducted on cube specimens to determine the compression strength of paste specimens at ages of 3, 7, 14, and 28 days. The loading rate was set as 1 kN/s. To test the aggregate-cement paste bond strength, a custom-made clamp was employed to fix the cylinder samples, as shown in **Fig. 1**. Uniaxial tensile test was performed on a hydraulic universal material testing machine (MTS, model 810) and the loading rate is set as 0.3 mm/min and each group consists of at least 3 samples.

To examine the carbonation profile along the cement paste depth, the 25 mm^3 cubes were prepared. After demoulding, the side surface and bottom surface were covered with paraffin to allow the one-way CO_2 penetration via top surface. The cubes were then moved to carbonation chamber for 28 days. After which, the paraffins were removed from sample surface and the samples were cut into 5-mm-thick slices from top to bottom. The slices from the same depth were immersed in isopropanol for 3 days to quench the hydration, followed by drying at 40 °C for 2 days. The collected slices were ground into powder that can pass through the 75-μm sieve, and most of the PVA fibers were screened out at the same time. The collected powders were subjected to XRD and TGA characterizations.

Table 1: Mix proportions and flowability of RMC and PC-based paste

Mix ID	MgO	Cement	Water	$Na(PO_4)_6$	SP	PVA fiber (vol.%)	Flowability
RMC	1	-	0.76	0.02	-	2	182.5
PC	-	1	0.32	-	0.01	2	185

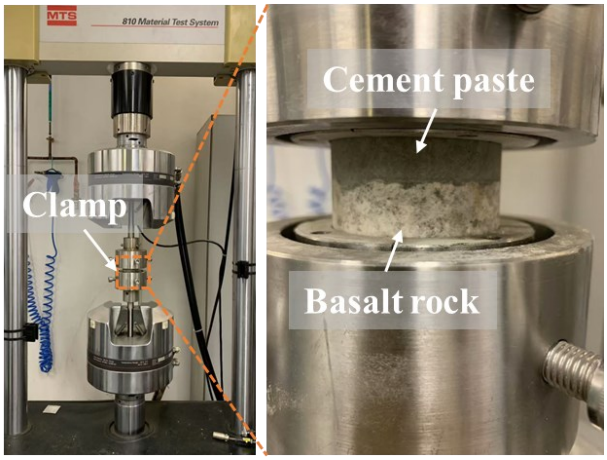

Figure 1: Setup of the tensile test.

3 RESULTS AND DISCUSSIONS

3.1 Mechanical strength

Fig. 2 shows the compression strength (f_c) of RMC and PC-based paste. The RMC under sealed curing exhibits the lowest f_c, with marginal increase from 3 MPa to 3.6 MPa as the curing time extends from 3 days to 28 days. Such low f_c is ascribed to the weak interaction among the brucite plates. Upon applying the carbonation curing to RMC, the f_c was increased dramatically. The maximum f_c is observed in RMC after 14 days carbonation curing, which is more than 10 times that of RMC under sealed curing (e.g., 37.4 MPa vs. 3.6 MPa). This comparison highlights the heavy dependency of RMC on CO_2 curing for strength gain. However, a slight reduction in f_c can be noted when the curing period is extended to 28 days, perhaps due to the carbonation-induced microcracking within RMC paste [15].

For PC-based paste under sealed curing, it demonstrates a steady improvement in f_c with the progression of curing time, and the f_c of PC is prominently higher compared with RMC, e.g., 44.4-56.9 MPa vs. 3.0-3.6 MPa. Interestingly, carbonation curing of PC leads to a slight decrease in f_c, demonstrating that the strength gain of PC relies on the hydration process and the formation of C-S-H gel and Portlandite. According to previous studies [16-18], the C-S-H gel is prone to decomposition under carbonation curing, forming the silica gel and leading to coarsening effect in pore structure, which may compromise the strength. However, the f_c of PC is still about 39% higher than that of RMC after 28-day carbonation curing.

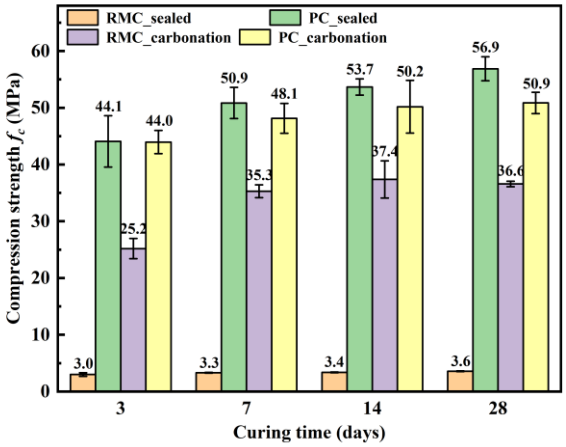

Figure 2: Compression strength of RMC and PC-based paste.

Fig. 3a and **3b** illustrate the load-displacement (P-u) curves of RMC and PC-based composites. Due to the perturbance of load cell during tensile loading, the P-u curves was linearly fitted for clear display. As expected, the load peak (P_{max}) of RMC specimens continuously increases with the extension in carbonation period, and the RMC specimens under sealed curing exhibits the lowest tensile load. Likewise, the P_{max} of PC specimens also increase with the carbonation curing go onwards, whereas the maximum P_{max} is spotted in PC specimens under sealed curing. The aggregate-cement paste bond strength (f_b) was calculated by **Eq. (1)**, S is the area of aggregate-cement paste interface.

$$f_b = P_{max}/S \quad (MPa) \qquad (1)$$

The calculated f_b is shown in **Fig. 3c**, the f_b of RMC under carbonation curing demonstrates a significant rise from 0.11 MPa to 0.94 MPa as the curing duration extends from 3 days to 28 days. As a comparison, the RMC after 28-day sealed curing exhibits the lowest f_b of 0.06 MPa, suggesting the brucite is unable to provide sufficient chemical interaction between cement paste and aggregate. Regarding the PC specimens under carbonation curing, the f_b also showcases a

steadily enhancement with curing duration progresses. However, after 7-day carbonation, the increase in f_b is insignificant, e.g., from 1.82 MPa to 1.95 MPa. The highest f_b of 2.12 MPa is seen in PC after 28-day sealed curing. This phenomenon reveals that the carbonation curing also slightly deteriorates the chemical interaction between PC and aggregate. By and large, the f_b of PC is remarkably higher than that of RMC, e.g., the f_b of PC is more than doubled that of RMC after 28-day carbonation.

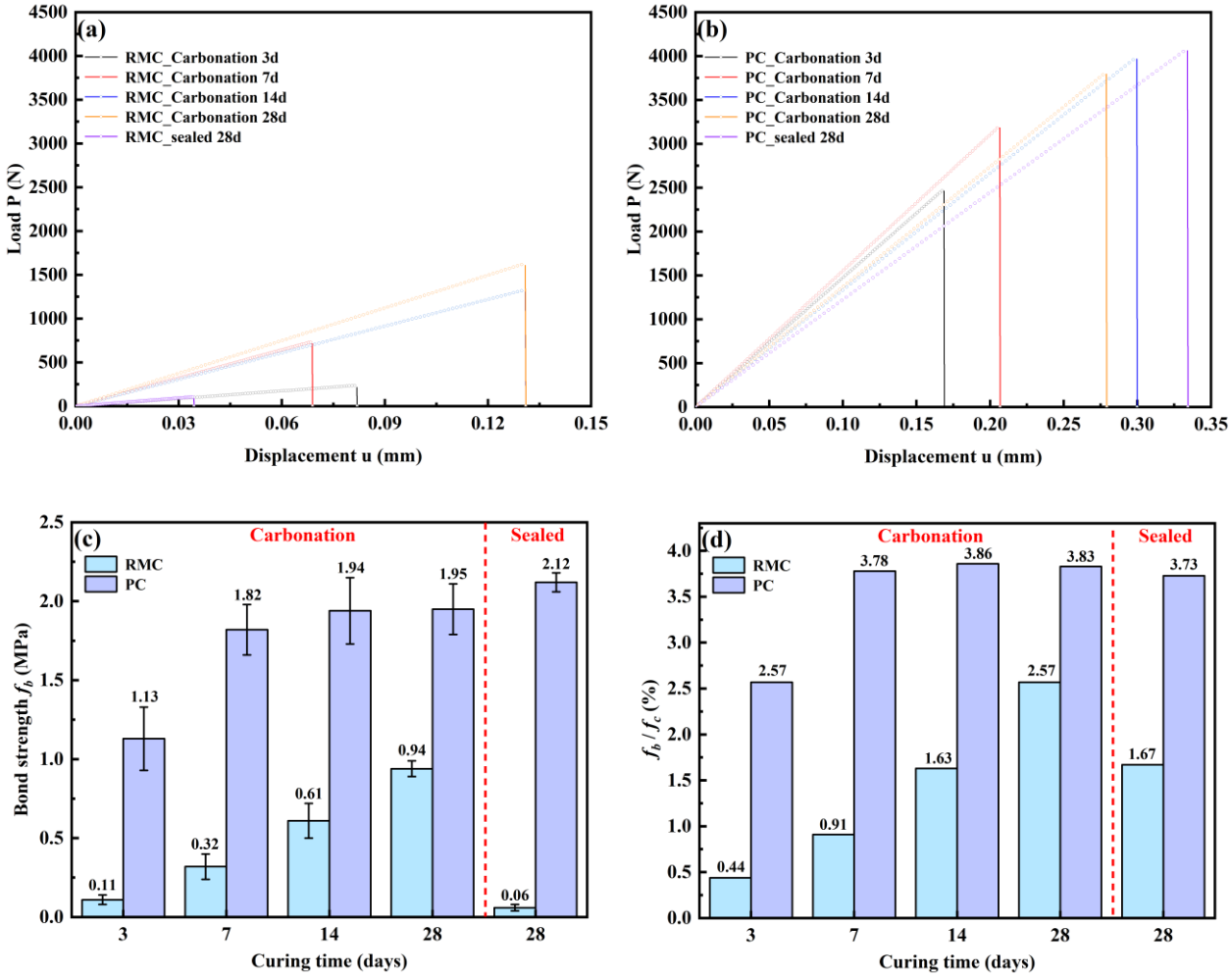

Figure 3: Representative load (P)-displacement (u) curves of (a) RMC and (b) PC-based composites, (c) is the calculated the aggregate-cement paste bond strength, (d) is the bond strength-compression strength (f_b/f_c) ratio.

Fig. 3d shows the bond strength-compression strength (f_b/f_c) ratio. As reported in previous literatures [7, 19], the aggregate-cement paste bond strength is proportional to the matrix mechanical strength and micro-physical properties of ITZ. The trend is also observed in PC specimens, after 7-day carbonation or 28-day sealed curing, the f_b/f_c ratio almost remains unchanged, e.g., 3.73-3.86. The stable f_b/f_c ratio indicates the chemical interaction between the aggregate and cement paste is highly related with the mechanical performance of cement paste. However, the RMC demonstrate a different trend in f_b/f_c ratio, it increases steadily from 0.44 to 2.57 with the carbonation duration extends from 3 days to 28 days. The unstable f_b/f_c ratio exactly manifests the particularity of carbonated RMC, which is pertinent with the change in chemical composition, e.g., conversion from brucite to HMCs. The brucite plates are connected with weak hydrogen bonds (bond energy of 21 kJ/mol [20, 21]) and are inferior in physical properties (e.g., the elastic modulus is only 2.5 GPa [22]), hence they are unable to provide strong interaction

with aggregate. By comparison, the HMCs are connected by Mg-O bonds (bond energy of 327 kJ/mol [23]) and have higher elastic modulus of 19.4 GPa [22]. Accordingly, the formation of HMCs significantly improves the chemical interaction with the aggregate.

Interestingly, the f_c of RMC is about 72% of the PC after 28-day carbonation, whereas the f_b is only 48% of the PC. Additionally, the f_b/f_c ratio of RMC is only 67% of the PC. These two values signify that the HMCs of RMC contributes less to the chemical interaction compared with the C-S-H gel of PC.

3.2 Carbonation profile

The XRD patterns of RMC specimens after 28-day carbonation and sealed curing are shown in **Fig. 4a**. The presence of unhydrated MgO (2θ=42.9°) and uncarbonated brucite (2θ=38.1°) can be observed in all specimens, while their intensity varies significantly. The intensity of brucite reflection increases with the depth, and the RMC under sealed curing has the most prominent brucite reflection. This observation implies that more brucite was converted into HMCs at the shallow regions (e.g., 0-5 mm). Carbonation of shallow regions would significantly densify the microstructure, which inhibits the further penetration of CO_2 into deep regions, causing a limited carbonation depth [6, 24]. Interestingly, the intensity of MgO reflection is stronger at the shallow regions, and the MgO reflection is almost invisible at the depth > 15 mm and RMC under sealed curing. The relatively low hydration degree of RMC at the shallow region is associated with the barrier effect of dense HMCs formed on the surface of MgO particles [25, 26]. Noticeably, the HMCs, such as nesquehonite (2θ=13.6°, 23.1°) and hydromagnesites (2θ=15.2°), can be explicitly observed at the depth of 0-5 mm, and the reflections of HMCs significantly declines at the depth of 5-15 mm. With the depth exceeds 15 mm or the RMC under sealed curing, almost no reflections associated with HMC are observed, indicating a low carbonation degree.

Fig. 4b presents the XRD pattern of PC specimens. The reflections belonging to Portlandite (2θ=18.1°) and unreacted clinker can be seen in all specimens. The intensity of Portlandite reflection increases with depth increases while the intensity of calcite reflection (2θ=23.1°) is more evident at the shallow regions. This comparison reveals that more Portlandite was converted into calcite at the shallow regions.

Fig. 5a shows the mass loss and heat evolution of RMC paste from 50°C to 1000°C. Obviously, the total mass loss is more pronounced at the shallow regions, and the smallest mass loss can be seen in RMC under sealed curing, which is attributed to the higher decomposition of HMCs at the shallow regions. Based on the endothermic peaks [2, 24], the chemical and physical changes of the hydrated and carbonated phases are assigned as follows: dehydration of water bonded to HMCs at 50-300°C; decomposition of uncarbonated brucite, dehydroxylation and minor decarbonation of HMCs at 300-450°C; major decarbonation of HMCs above 450°C.

At the depth of 0-5 mm, the endothermic peak corresponded to dehydration of HMCs at 115°C is quite prominent, its intensity decreases gradually with the depth increases, and almost disappears at the depth > 15 mm or the RMC under sealed curing. On the contrary, the endothermic peak representing the decomposition of brucite (320-420°C) is more pronounced in sealed RMC specimen and deep regions, suggesting that less brucite was converted to the HMCs. The endothermic peak slightly shifted from 385°C to 395°C, which is due to the barrier effect of HMCs on brucite surface or the decomposition of amorphous HMCs [25]. The endothermic peaks associated with decarbonation of HMCs are more conspicuous at the shallow regions, which complies with the XRD results. These observations demonstrate the uneven distribution of carbonation along the depth of RMC, which determines the microstructure and mechanical performance.

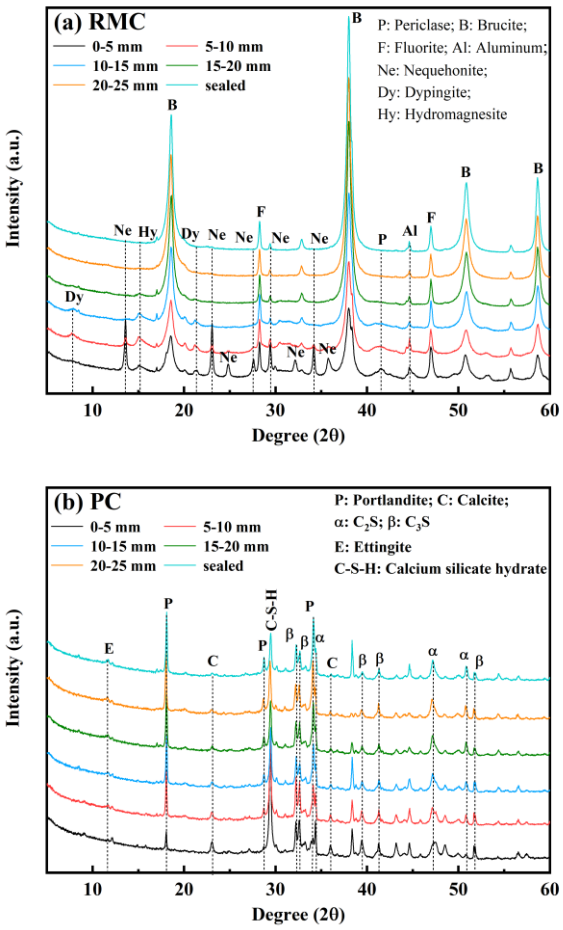

Figure 4: XRD patterns of (a) RMC and (b) PC at different depths after 28-day carbonation and sealed curing.

Fig. 5b illustrates the mass loss and heat evolution of PC paste from 50°C to 1000°C. The endothermic peak at around 80°C is responsible for the water loss of ettringite. The endothermic peak between 400°C and 450°C belongs to the dehydration of Portlandite, and the peak at 450°C-800°C is pertinent to the decarbonation of calcite. The changes of intensity of these two peaks along the depth are opposite, the intensity of endothermic peak associated with dehydration of Portlandite increases with the depth while the intensity of decarbonation peak decreases with the depth. This reverse trend discloses that more Portlandite was carbonized into calcite at the shallow regions.

The fraction of unhydrated MgO and uncarbonized brucite, and the mass losses of RMC specimens at different temperatures are listed in **Table 2**. The carbonation degree (D_{CO2}) of RMC is determined by **Eq. (2)**, where P_{CO2} represents the percentage of sequestrated CO_2 calculated by subtracting the weight loss of H_2O from the total weight loss between 300°C and 1000°C, and R_{MgO} is residual MgO after 1000°C calcination. The mass losses of PC specimens at different temperatures are also included in **Table 2**. The mass loss at 450°C-1000°C was utilized to calculate the carbonation degree.

$$D_{CO2}=P_{CO2}/R_{MgO} \quad (2)$$

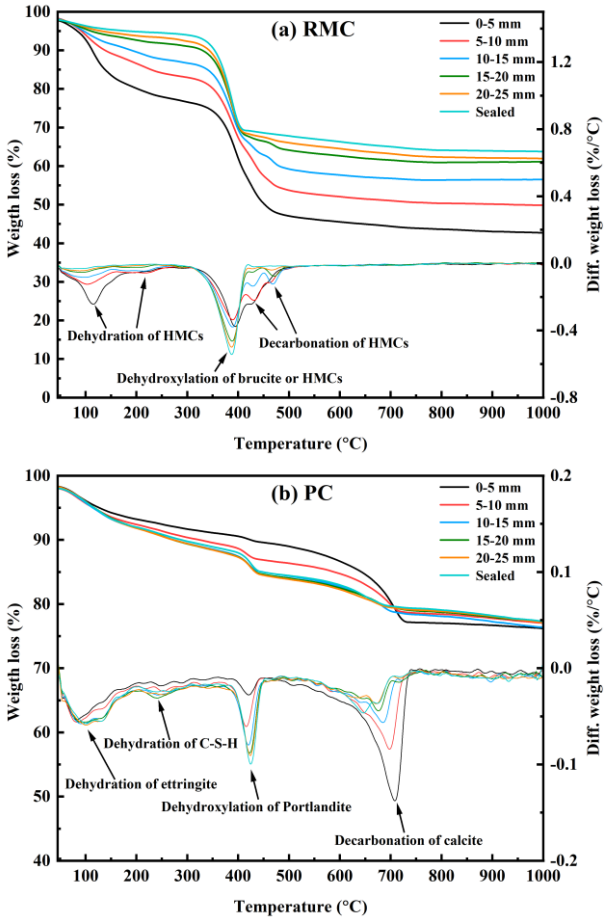

Figure 5: TGA curves of (a) RMC and (b) PC at different depths after 28-day carbonation and sealed curing.

As expected, for both of RMC and PC specimens, the shallow regions have the maximum carbonation degree, which gradually decreases with the depth increases. When the depth increases to 15 mm, the carbonation degree is comparable to the specimens under sealed curing, indicating a marginal carbonation degree. Compared with

PC-based paste, the RMC-based paste displays a significantly higher carbonation degree at the depth of 0-10 mm, e.g., 0.366-0.473 of RMC vs. 0.098-0.134, manifesting that the RMC holds greater potential to be a carbon reservoir than that of PC.

The contribution of carbonation to the aggregate-cement paste bond strength (ξ) was calculated as follows:

$$\overline{C} = \sum_{i=1}^{5} V_i C_i \quad (3)$$

$$\xi = \frac{\overline{C}}{f_{bc} - f_{bs}} \times 100\% \quad (4)$$

where the $\overline{C}$ is the average carbonation degree of the cylinder paste specimens, V_i is the volume fraction at the depth of i (e.g., 0-5 mm), C_i is carbonation degree at the depth of i (e.g., 0-5 mm). The f_{bc} and f_{bs} are the bond strength after 28-day carbonation and sealed curing, respectively. The calculated ξ value is shown in **Fig. 6**, the ξ value of RMC is 35.3%/MPa while the ξ value of PC is -61.7%/MPa. This comparison discloses that the bond strength of RMC is highly dependent on the carbonation while carbonation of PC is detrimental to the aggregate-cement paste bond strength. In addition, the ξ value of RMC implies that its bond strength can be further enhanced with the carbonation degree increases, theoretically, the bond strength of RMC can surpass the PC if the carbonation degree reaches 70%.

Table 2: Mix proportions and flowability of RMC and PC-based paste

Specimen	Depth	XRD		TGA			Carbonation degree
		MgO	$Mg(OH)_2$	50-300°C	300-450°C	450-1000°C	
RMC	0-5 mm	0.103	0.443	20.98	26.28	7.65	0.473
	5-10 mm	0.076	0.481	15.17	25.50	7.66	0.366
	10-15 mm	0.059	0.710	11.37	23.81	6.39	0.145
	15-20 mm	0	0.848	6.71	24.59	5.36	0.061
	20-25 mm	0	0.886	5.60	24.85	5.56	0.057
	Sealed	0	0.904	3.86	25.36	3.88	0.034
PC	0-5 mm	-	-	6.58	2.09	13.42	0.134
	5-10 mm	-	-	7.58	3.51	9.81	0.098
	10-15 mm	-	-	8.56	4.48	8.65	0.087
	15-20 mm	-	-	8.69	4.76	7.40	0.074
	20-25 mm	-	-	8.79	4.93	7.42	0.074
	Sealed	-	-	8.22	4.83	7.66	0.076

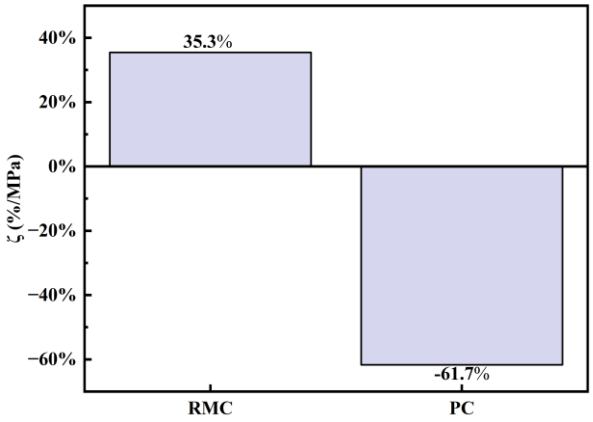

Figure 6: Contribution of carbonation to the aggregate-cement paste bond strength.

4 CONCLUSIONS

This work compared the compression strength, aggregate-cement paste bond strength, and carbonation profile between the RMC and PC. Mechanical performances results revealed that both the paste strength and bond strength of RMC are heavily dependent on the carbonation curing, the mechanical strength of carbonated RMC is more than 10 times that of RMC under sealed curing. By contrary, carbonation curing slightly compromises the mechanical properties of PC. The chemical characterization shows an uneven distribution of carbonation degree along the depth, the carbonation degree significantly declines with the depth, and the carbonation degree at the deep regions (e.g., depth > 15 mm) is comparable to the specimens under sealed curing. Building upon the mechanical performance and carbonation profile, the contribution of carbonation to aggregate-cement paste bond strength was calculated and compared, suggesting that the RMC holds great potential to achieve higher bond strength than that of PC only upon the carbonation degree is further enhanced.

REFERENCES

[1] H. Wang, S. Liang, X. Zhou, P. Hou, X. Cheng, Regulating hydration and microstructure development of reactive MgO cement by citric acids, Cement and Concrete Composites (2024) 105832.
[2] C. Pan, Y. Song, J. Wang, S. Zhan, C. Unluer, S. Ruan, Unlocking the role of recycled aggregates in the performance enhancement and CO_2 capture of reactive magnesia cement formulations, Cement and Concrete Research 168 (2023) 107148.
[3] N. Dung, C. Unluer, Carbonated MgO concrete with improved performance: The influence of temperature and hydration agent on hydration, carbonation and strength gain, Cement and Concrete composites 82 (2017) 152-164.
[4] N. Dung, C. Unluer, Development of MgO concrete with enhanced hydration and carbonation mechanisms, Cement and Concrete Research 103 (2018) 160-169.
[5] N. Dung, C. Unluer, Influence of nucleation seeding on the performance of carbonated MgO formulations, Cement and Concrete Composites 83 (2017) 1-9.
[6] B. Wu, S. Qin, J. Qiu, Effect of hollow natural fiber (HNF) content on the CO_2 diffusion, carbonation, and strength development of reactive magnesium cement (RMC)-based composites, Cement 16 (2024) 100102.
[7] M. Jebli, F. Jamin, E. Malachanne, E. Garcia-Diaz, M.S. El Youssoufi, Experimental characterization of mechanical properties of the cement-aggregate interface in concrete, Construction and Building Materials 161 (2018) 16-25.
[8] Q. Chen, J. Zhang, Z. Wang, T. Zhao, Z. Wang, A review of the interfacial transition zones in concrete: Identification, physical characteristics, and mechanical properties, Engineering Fracture Mechanics 300 (2024) 109979.
[9] W.A. Tasong, C.J. Lynsdale, J.C. Cripps, Aggregate-cement paste interface: Part I. Influence of aggregate geochemistry, Cement and concrete research 29(7) (1999) 1019-1025.
[10] L. Hong, X. Gu, F. Lin, Influence of aggregate surface roughness on mechanical properties of interface and concrete, Construction and Building Materials 65 (2014) 338-349.
[11] D. Seo, H. Choi, Effects of the old cement mortar attached to the recycled aggregate surface on the bond characteristics between aggregate and cement mortar, Construction and Building Materials 59 (2014) 72-77.
[12] Y. Wong, L. Lam, C.S. Poon, F. Zhou, Properties of fly ash-modified cement mortar-aggregate interfaces, Cement and Concrete Research 29(12) (1999) 1905-1913.
[13] X. Wang, S. Dong, A. Ashour, W. Zhang, B. Han, Effect and mechanisms of nanomaterials on interface between aggregates and cement mortars, Construction and Building Materials 240 (2020) 117942.
[14] L. Pu, S. Ruan, C. Pan, Y. Song, F. Zhou, J. Lai, K. Qian, Q. Li, Pore structures and interfacial properties between hydrated magnesia carbonates-modified recycled aggregate and reactive magnesia paste, Construction and Building Materials 404 (2023) 133190.
[15] R. Hay, K. Celik, Hydration, carbonation, strength development and corrosion resistance of reactive MgO cement-based composites, Cement and Concrete Research 128 (2020) 105941.
[16] B. Šavija, M. Luković, Carbonation of cement paste: Understanding, challenges, and opportunities,

Construction and Building Materials 117 (2016) 285-301.
[17] V. Ngala, C. Page, Effects of carbonation on pore structure and diffusional properties of hydrated cement pastes, Cement and concrete research 27(7) (1997) 995-1007.
[18] L. Pu, C. Unluer, Investigation of carbonation depth and its influence on the performance and microstructure of MgO cement and PC mixes, Construction and Building Materials 120 (2016) 349-363.
[19] Y. Tu, H. Yu, H. Ma, W. Han, Y. Diao, Experimental study of the relationship between bond strength of aggregates interface and microhardness of ITZ in concrete, Construction and Building Materials 352 (2022) 128990.
[20] N.N. Greenwood, A. Earnshaw, Chemistry of the Elements, Elsevier 2012.
[21] P. D'Arco, M. Causà, C. Roetti, B. Silvi, Periodic Hartree-Fock study of a weakly bonded layer structure: Brucite $Mg(OH)_2$, Physical Review B 47(7) (1993) 3522.
[22] N. Dung, A. Lesimple, R. Hay, K. Celik, C. Unluer, Formation of carbonate phases and their effect on the performance of reactive MgO cement formulations, Cement and Concrete Research 125 (2019) 105894.
[23] Y.-R. Luo, Comprehensive handbook of chemical bond energies, CRC press 2007.
[24] N. Dung, R. Hay, A. Lesimple, K. Celik, C. Unluer, Influence of CO_2 concentration on the performance of MgO cement mixes, Cement and Concrete Composites 115 (2021) 103826.
[25] R. Hay, B. Peng, K. Celik, Filler effects of $CaCO_3$ polymorphs derived from limestone and seashell on hydration and carbonation of reactive magnesium oxide (MgO) cement (RMC), Cement and Concrete Research 164 (2023) 107040.
[26] B. Wu, Y.W. Chung, Y. Tang, J. Qiu, Effect of internal moisture content (IMC) on the CO_2 sequestration efficiency of hollow natural fiber (HNF)-reinforced reactive magnesia cement (RMC) composites, Construction and Building Materials 428 (2024) 136339.